



# HHS Public Access

Author manuscript

*Nat Cell Biol.* Author manuscript; available in PMC 2012 November 01.

Published in final edited form as:

*Nat Cell Biol.* ; 14(5): 518–525. doi:10.1038/ncb2467.

## Drosophila Src regulates anisotropic apical surface growth to control epithelial tube size

Kevin S. Nelson<sup>1</sup>, Zia Khan<sup>2,3,†</sup>, Imre Molnár<sup>4</sup>, József Mihály<sup>4</sup>, Matthias Kaschube<sup>2,5,‡</sup>, and Greg J. Beitel<sup>1,\*</sup>

<sup>1</sup>Department of Molecular Biosciences and Robert H. Lurie Comprehensive Cancer Center, Northwestern University, Evanston, IL 60208, USA

<sup>2</sup>Lewis-Sigler Institute for Integrative Genomics, Princeton University, Princeton, NJ, 08542, USA

<sup>3</sup>Department of Computer Science, Princeton University

<sup>4</sup>Institute of Genetics, Biological Research Centre, Hungarian Academy of Sciences, Temesvari krt. 62, Szeged, 6726 Hungary

<sup>5</sup>Department of Physics, Princeton University

### Abstract

Networks of epithelial and endothelial tubes are essential for the function of organs such as the lung, kidney, and vascular system. The sizes and shapes of these tubes are highly regulated to match their individual functions. Defects in tube size can cause debilitating diseases such as polycystic kidney disease (PKD) and ischemia<sup>1,2</sup>. It is therefore critical to understand how tube dimensions are regulated. Here we identify the tyrosine kinase Src as an instructive regulator of epithelial tube length in the *Drosophila* tracheal system. Loss-of-function *Src42* mutations shorten tracheal tubes while *Src42* over-expression elongates them. Surprisingly, *Src42* acts distinctly from known tube size pathways and regulates both the amount of apical surface growth and, with the conserved formin *dDaam*, the direction of growth. Quantitative 3-D image analysis reveals that *Src42* and *dDaam* mutant tracheal cells expand more in the circumferential than the axial dimension, resulting in tubes that are shorter in length – but larger in diameter – than WT tubes. Thus, *Src42* and *dDaam* control tube dimensions by regulating the direction of anisotropic growth, a mechanism that has not previously been described.

---

Users may view, print, copy, download and text and data- mine the content in such documents, for the purposes of academic research, subject always to the full Conditions of use: [http://www.nature.com/authors/editorial\\_policies/license.html#terms](http://www.nature.com/authors/editorial_policies/license.html#terms)

\*Author for correspondence: Greg J. Beitel, Hogan Hall, Rm. 2-100, Northwestern University, Evanston, IL 60208, U.S.A., [beitel@northwestern.edu](mailto:beitel@northwestern.edu), Ph: (847) 467-7776, FAX: (847) 467-1380.

†Current address: Department of Human Genetics, University of Chicago, Chicago, IL 60637, USA

‡Current address: Frankfurt Institute for Advanced Studies and Department of Computer Science and Mathematics, Johann Wolfgang Goethe University, Frankfurt am Main, Germany

### Author Contributions

KSN performed all experiments, ZK generated and analyzed individual DT cell quantifications, IM generated the UAS-Flag-dDaam construct and the dDaam antibody, KSN, ZK, MK and GJB designed and interpreted the experiments, and KSN, ZK, JM, MK and GJB wrote the paper.

### Competing financial interests

The authors declare no competing financial interests.

The *Drosophila* tracheal system is a gas exchange organ that arises from clusters of epithelial cells that invaginate, branch, and interconnect to form a network of tubes. After network formation, tracheal lumens dramatically increase their diameters and lengths<sup>3</sup>. Importantly, these expansions result exclusively from changes in cell shape and apical surface area since tracheal cell number does not change during expansion<sup>3,4</sup>.

Multiple cellular processes are known to control tracheal tube size. Overexpression of the apical determinant Crumbs (Crb) increases both the length and diameter of late stage tracheal tubes<sup>5</sup> and loss of the basal polarity protein Scribbled (Scrib) increases tube length<sup>5,6</sup>. Mutations in planar cell polarity (PCP) genes also cause modest tube over-elongation resulting from increased apical cell surface<sup>7</sup>. The best-characterized size control pathway involves the apical extracellular matrix (aECM) whose assembly depends on a cell-cell junction termed the septate junction (SJ). After tracheal metameres fuse, a chitin-based aECM is secreted apically into the tracheal lumen<sup>8–10</sup>. Putative chitin deacetylases Verm and Serp are secreted into the lumen to regulate aECM organization and are required to prevent over-elongation of tracheal tubes<sup>11,12</sup>. Basolateral SJs direct apical secretion of Verm and Serp via an uncharacterized pathway<sup>12</sup>. Consequently, mutations in almost all SJ components also cause tube over-elongation<sup>6,13–15</sup>. To date, mutations that dramatically shorten the length of late-stage embryonic tracheal tubes have not been reported. Further, with the possible exception of Crb, the currently identified size-control proteins act as “permissive” rather than “instructive” factors, since their over-expression does not cause phenotypes opposite to their loss-of-function phenotypes<sup>12,14,16</sup>.

Src-family kinases (SFKs)<sup>17</sup> have been implicated in controlling the size of mammalian epithelial and endothelial tubes, though the mechanisms by which they do so have not been elucidated<sup>18,19</sup>. We therefore examined the tracheal system of *Drosophila* embryos homozygous for null mutations in either of the two known SFKs, *Src42* and *Src64*. Neither zygotic nor maternal/zygotic (M/Z) *Src64* mutants showed tracheal defects or genetic interactions with a mutation in *ATPa* that elongates tracheal tubes<sup>13</sup>, and *Src64* was not detected in tracheal cells using immunohistochemistry (Fig. S1 online). In contrast, by late embryogenesis (stage 16), zygotic loss of *Src42* caused the dorsal trunk (DT), the largest and most easily analyzed tracheal tube, to be ~27% shorter than WT controls (Fig. 1b, d, q) and to have a “stretched” appearance in which the angle of the anterior transverse connective (TC) 1 relative to the DT was significantly increased in *Src42* mutants over WT controls (Fig. 1e, f) and the normal ventral curve of the posterior DT metamere 10 was absent (Fig. 1g, h). Measurements revealed that *Src42* elongation defects become apparent after tracheal metameres fuse midway through embryogenesis (Fig. 1a,c; 2jj) as the DT begins elongating<sup>3</sup>. Importantly, the elongation defect of *Src42* mutants is independent of cell number, since *Src42* and WT DTs have the same number of cells (metamere 8: WT =  $24.1 \pm 1.6$ , *Src42* =  $24.3 \pm 2.1$ ,  $p = 0.24$ ,  $n = 8$ ). These observations identify *Src42* as one of the first genes required for increasing the length of late-stage embryonic trachea.

As SFKs can mediate cellular functions independent of their tyrosine kinase activity<sup>20,21</sup>, we expressed either a WT (*Src42*<sup>WT</sup>)<sup>22</sup> or a kinase-dead form of *Src42* (*Src42*<sup>KM</sup>)<sup>23</sup> specifically in the trachea<sup>24</sup> of *Src42* mutants. *Src42*<sup>WT</sup> could completely rescue the DT elongation defect of *Src42* mutants while *Src42*<sup>KM</sup> could not, despite similar levels of expression (Fig.

li–n, q). Furthermore, over-expression of Src42<sup>KM</sup>, which acts as a dominant negative in other systems<sup>23,25</sup>, shortened DTs (Fig. 1o, r). Together, these results indicate that the kinase activity of Src42 is required autonomously in trachea for DT elongation.

Over-expression of Src42<sup>WT</sup> in the tracheal system resulted in severe DT fusion defects that precluded analysis of DT length (data not shown). However, over-expressing Src42<sup>WT</sup> in a *Src42* heterozygote did not disrupt fusion and increased tracheal DT length by ~8% (Fig. 1p, r). Combinations of loss-of-function *Src42* alleles and over-expression constructs produced an allelic series in which the tracheal length ranged from ~27% too short to ~8% too long (Fig. 1r). Thus, Src42 acts instructively to regulate tube size.

Because the kinase activity of Src42 is required for regulating tracheal length, we determined the subcellular localization of activated (phosphorylated Tyr-400) Src42 (pSrc) in tracheal cells. As reported previously<sup>23</sup>, while endogenous Src42 localizes throughout the plasma membrane of all DT cells (Fig. 1k), activated Src42 largely co-localizes with DE-cadherin (DE-cad) at the adherens junction (AJ) (Fig 2a–c, arrows) and partially co-localizes with Crb at the subapical membrane (Fig 2d–f, arrowheads). Activated Src42 does not co-localize with SJs (Fig. 2g, h). Notably, a large fraction of phosphotyrosine (pTyr) immunostaining that normally localizes to the AJ and subapical membrane (Fig. 2m, n) is absent in *Src42* mutants (Fig. 2o, p), while Src42 over-expression results in a dramatic increase in pTyr content (Fig 2q, r). Thus, Src42 appears to be either directly or indirectly required for the majority of tyrosine phosphorylation in the tracheal system. Given the critical role pTyr is thought to play in junctional and cytoskeletal assembly and turnover<sup>23,26,27</sup>, *Src42* mutations have unexpectedly mild effects on tracheal morphology.

The elongated tracheal phenotype caused by Src42 over-expression is highly similar to that caused by polarity, SJ, and aECM loss-of-function mutations (Fig. 2u and <sup>5,6,11,12,14,16</sup>). To investigate whether Src42 acts in these pathways, we performed genetic epistasis experiments using null alleles of *Src42* and several polarity, SJ, and aECM genes. Unfortunately, double mutant combinations of *Src42* and the polarity genes *scrib*, *yrt*, and *lgl* resulted in severe defects in embryogenesis, making clear analysis of DT length difficult. However, the short-tracheal phenotype of *Src42* was epistatic to all tested SJ and aECM mutations (Fig. 2s–v, aa, and Fig. S2m–p and Table S1a online). Importantly, *Src42* suppressed over-elongation without improving aECM or SJ organization (Fig. 2w–z and S2a–p online). Consistent with this, Src42 over-expression resulted in DT over-elongation without significantly disrupting SJ integrity or aECM organization (Fig. S2q–t online). These results indicate that Src42 acts either downstream of the SJ/aECM tube size control pathways or independently in a parallel pathway.

To distinguish between “downstream” and “in parallel”, we assessed Src42 activity in SJ, aECM, and polarity mutants. If Src42 acts downstream of the SJ/aECM or polarity pathways, loss-of-function mutations in SJ, aECM or polarity genes should increase Src42 activity. However, we were unable to detect any changes in the levels or localization of pSrc, pTyr, or total Src42 in any tube expansion mutants (Fig. 2bb–ee and S2u–bb online), although elevated pSrc was readily detected when Src42 was over-expressed in the tracheal system (Fig. 2k, l). Moreover, over-expression of Src42 in a *nrv2* null background (an

essential SJ gene) resulted in a dramatically enhanced tracheal phenotype consisting of loss of luminal 2A12 and a cystic lumen (Fig. 2ff–ii) suggesting that *Src42* and *nrv2* do not function in the same linear pathway. Consistent with this, *Src42* and *nrv2* act at separable developmental times. *Src42* is required to initiate elongation between hours 10 and 12 of development, while *nrv2* is required to restrict tube length after hour 12 (Fig. 2jj).

We also asked whether *Src42* acts in the canonical PCP pathway to control tracheal length<sup>7</sup>. However, in contrast to *Src42*, mutations in the PCP genes *dsh*, *fz*, and *sano* cause elongated trachea (Fig. S3m and<sup>7</sup>), and the short phenotype of *Src42* was completely epistatic to all tested PCP mutants (Table S1a online). Further, *sano* and *dsh* mutants did not show any changes in the levels of activated *Src42* (Fig. S2u–x online and data not shown) and *Src42* mutations did not alter the planar polarization of wing hairs, thorax bristles, or denticle belts (Fig. S3a–l online). Specific expression of a dominant negative *Src42* construct in the thorax also did not affect planar polarization (Fig. S3h online) and caused only very subtle effects when expressed in a specific wing region (Fig. S3d' online). Finally, while *Dsh* and other PCP genes have a planar polarized localization in other epithelia such as the epidermis, their distribution appears uniform in the trachea (Fig. S3q–t and<sup>7</sup>). Thus, *Src42* acts either downstream or in parallel to PCP genes to control tube size. Together, these data indicate that *Src42* acts in a pathway separate from known tracheal tube size control genes.

To understand the cellular functions of *Src42* in tube size control, we investigated the morphology of WT and *Src42* DT cells. We reasoned that short trachea could result either from a general failure to expand apical surface or from a failure to direct surface expansion anisotropically along the length of the tube, which would result in shorter but fatter tubes that were inappropriately expanded along the circumferential axis (Fig. 3a). To distinguish between these models, we measured both the length and diameter of WT and *Src42* metamere 8 lumens. Interestingly, while *Src42* lumens were ~37% shorter than WT controls (Fig. 3b,c,d), they were also ~11% larger in diameter (Fig. 3e). We calculated that the total apical surface area (ASA) of *Src42* metameres is reduced by ~30% (Fig. 3f, see Materials and Methods), indicating that *Src42* is required for increasing apical surface. However, the increased lumen diameter of *Src42* mutants indicates that *Src42* is also required for directing available surface expansion along the axial dimension.

To quantify these results at the single cell level, we determined ASA, axial length, aspect ratio, and cell orientation using 3D reconstructions of individual WT and *Src42* tracheal cells (Fig. 3g–i and Materials and Methods). As observed for the whole metamere, the median ASA and axial length of individual *Src42* cells was smaller than WT cells (Fig. 3j, k). Interestingly, despite the smaller size of *Src42* cells, the median aspect ratios of WT and *Src42* cells was not significantly different (Fig. 3l). However, the median angle of the longest cell dimension relative to the longitudinal tube axis was closer to 90° in *Src42* than WT DT cells (Fig. 3m). Together, these data confirm that *Src42* is required for controlling the amount of apical surface expansion, and for directing available expansion anisotropically along the longitudinal axis of the tube. These results establish that epithelial tube size can be controlled by regulated anisotropic growth of the apical surface (Fig. 3a, Model 2).

To define the molecular mechanisms by which Src42 acts, we tested loss-of-function mutations in candidate Src interactors for a short tracheal phenotype (Table S1b online). We found that *dDaam*, a conserved diaphanous-related formin that has been shown to bind vertebrate Src<sup>28</sup>, displayed a mild, but significant short tracheal phenotype near the end of embryogenesis (stage 16) (Fig. 4m, 5l). Shortening was more apparent after hatching (Fig. 4a–c), raising the possibility that the weaker embryonic phenotype was due to maternal *dDaam* (failure of *dDaam* M/Z embryos to cellularize<sup>30</sup> precludes a direct test of this possibility). Like *Src42*, *dDaam* acts autonomously in the tracheal system since tracheal expression of Flag-tagged *dDaam* fully rescued the shortened DT of *dDaam* mutants (Fig. 4c, f). Remarkably, despite only causing modest reductions in DT length at embryonic stage 16, zygotic *dDaam* mutations were still able to completely suppress the over-elongation of SJ, aECM, apico-basal and PCP mutants (Fig. 4g–l and Table S1a online). Further, whereas *Src42; scrib* mutants had gross embryonic defects, *dDaam; scrib* mutants underwent largely normal development and had trachea with the *dDaam* short tracheal phenotype (Fig. 4n, o and Table S1a online). Thus, dDaam appears to act downstream or in parallel to all characterized tracheal tube size control pathways.

Using quantitative imaging, we determined that, as in *Src42* mutants, the apical surfaces of *dDaam* tracheal cells were misoriented, over-expanding in the circumferential direction to produce lumens that were shorter but larger in diameter (Fig. 4p–r, t–y). However, unlike *Src42* mutants, the apical surface of metamere 8 and the median apical surface of individual tracheal cells were not dramatically altered in *dDaam* mutants (Fig. 4s, v). Thus, dDaam is required to orient apical surface growth, but is either not required to control the amount of expansion or there is sufficient maternal dDaam to allow normal apical surface expansion.

The similar tracheal phenotypes of *Src42* and *dDaam* mutants suggested they act in the same pathway to control anisotropic surface growth. Consistent with this possibility, the short tracheal phenotype of the *dDaam; Src42* double mutant was not enhanced compared to the *Src42* single mutant, which is shorter than the *dDaam* mutant (Fig. 5l). In addition, dDaam colocalizes with pSrc at the AJ and subapical membrane of DT cells (arrows in Fig. 5a–c) and Src42 co-immunoprecipitates with dDaam from embryo lysates (Fig. 5d). Further, loss of *dDaam* decreased apical pSrc levels in DT cells (Fig. 5g, j, k), suggesting that dDaam acts upstream of Src42 in regulating tube-size. This is consistent with work in mammalian systems showing that Dia-related formins activate Src by binding to the auto-inhibitory SH3 domain<sup>28,31,32</sup>. Interestingly, though there were no obvious changes in the localization or levels of Src42 in *dDaam* mutants (Fig. 5f, i, k), the apical circumferential rings of dDaam were coarser and more broadly spaced in *Src42* mutant trachea (Fig. 5e, h), further evidencing functional interactions of these proteins.

Importantly, *dDaam* mutations do not completely eliminate phospho-Src staining. This result suggests that dDaam does not regulate all pools of Src42 in tracheal cells, which could explain why *Src42* mutants cause defects in both surface growth and orientation of growth, whereas dDaam mutations affect only orientation of growth. Consistent with this possibility, over-expression of Src42 in *dDaam* trachea caused marked excess growth in the circumferential direction, dramatically increasing tube diameter without increasing length (Fig. S4 online). Together, these results support a model in which Src42 regulates surface

expansion in a process that does not require dDaam, and that dDaam and Src42 act together in a complex that directs expansion along the longitudinal axis of the tube (Fig. 5m).

Given that Src42 and dDaam control directionality of cell growth in what is essentially a planar epithelium, we further investigated whether Src42 and dDaam act in the canonical PCP pathway. Although Src42 and dDaam do not act in PCP pathways outside the trachea (Fig S3a–l online), PCP genes could act upstream of Src42 and dDaam to control anisotropic growth in tracheal cells. Since a diagnostic feature of aberrant anisotropic growth is an increase in tube diameter when tube length is decreased, we determined tracheal diameter in embryos mutant for *ft*, a PCP gene whose loss causes short trachea. Tube diameter was unaltered (Fig. S3o, p online), indicating that canonical PCP genes act distinctly from Src42 and dDaam.

Surprisingly, loss of *Src42* or *dDaam* did not cause isotropic (equal in all dimensions) growth of apical surface. Instead, apical surface growth was dramatically reoriented along the circumferential tube axis (Fig. 3l,m; Fig. 4x,y). Thus, Src42 and dDaam are required for orienting anisotropic growth rather than being essential for anisotropic growth *per se*. Interestingly, homologs of both Src42 and dDaam have been shown to be required for mitotic spindle orientation<sup>33,34</sup>, suggesting that Src and Daam may have more broadly conserved roles in cellular anisotropy than have been previously suspected.

Our results reveal that *Drosophila* trachea use a mechanism of epithelial tube size control in which anisotropic growth of the apical surface drives increases in tube length or diameter. To our knowledge, this mechanism has not previously been described. Given that mammalian Src-family kinases have been implicated in control of tube size in the mammalian kidney<sup>19</sup> and vascular system<sup>18</sup>, and the general conservation of basic cellular processes, these results have important implications for control of tube size in other systems.

## Supplementary Material

Refer to Web version on PubMed Central for supplementary material.

## Acknowledgments

We thank Martin Zeeb and Eckhard Lammert for sharing unpublished results and comments on the manuscript; Rich Carthew, Sascha Hilgenfeldt and Andrew Dudley for insightful discussions, Bill Russin and the Northwestern Biological Imaging Facility for imaging support, Shigeo Hayashi, Alana O'Reilly, Tian Xu, the Bloomington Stock Center, and the Developmental Studies Hybridoma Bank for fly stocks and reagents, Mona Singh for technical advice, and Renée Robbins, Taneli Helenius, and Tom Krupinski for insightful comments on the manuscript. This work was supported by a predoctoral fellowship from the National Institutes of Health (NIH) Cellular and Molecular Basis of Disease training grant (T32 GM008061 to KSN), a Malkin Scholar Award (to KSN), an Achievement Rewards for College Scientists (ARCS) Award (to KSN), a grant from the Northwestern University Alumni Association (to GJB), NIH grant P50 GM 071508, PI: D. Botstein (ZK and MK), and OTKA grant K 82039 (to JM).

## References

1. Harris PC, Torres VE. Polycystic kidney disease. *Annu Rev Med.* 2009; 60:321–337. [PubMed: 18947299]

2. Requena L, Sanguenza OP. Cutaneous vascular anomalies. Part I. Hamartomas, malformations, and dilation of preexisting vessels. *J Am Acad Dermatol*. 1997; 37:523–549. quiz 549–552. [PubMed: 9344191]
3. Beitel GJ, Krasnow MA. Genetic control of epithelial tube size in the *Drosophila* tracheal system. *Development*. 2000; 127:3271–3282. [PubMed: 10887083]
4. Samakovlis C, et al. Development of the *Drosophila* tracheal system occurs by a series of morphologically distinct but genetically coupled branching events. *Development*. 1996; 122:1395–1407. [PubMed: 8625828]
5. Laprise P, et al. Epithelial polarity proteins regulate *Drosophila* tracheal tube size in parallel to the luminal matrix pathway. *Curr Biol*. 2010; 20:55–61. [PubMed: 20022244]
6. Wu VM, Schulte J, Hirschi A, Tepass U, Beitel GJ. Sinuous is a *Drosophila* claudin required for septate junction organization and epithelial tube size control. *J Cell Biol*. 2004; 164:313–323. [PubMed: 14734539]
7. Chung S, et al. Serrano (sano) functions with the planar cell polarity genes to control tracheal tube length. *PLoS Genet*. 2009; 5:e1000746. [PubMed: 19956736]
8. Tonning A, et al. A transient luminal chitinous matrix is required to model epithelial tube diameter in the *Drosophila* trachea. *Dev Cell*. 2005; 9:423–430. [PubMed: 16139230]
9. Moussian B, et al. *Drosophila* Knickkopf and Retroactive are needed for epithelial tube growth and cuticle differentiation through their specific requirement for chitin filament organization. *Development*. 2006; 133:163–171. [PubMed: 16339194]
10. Araujo SJ, Aslam H, Tear G, Casanova J. mummy/cystic encodes an enzyme required for chitin and glycan synthesis, involved in trachea, embryonic cuticle and CNS development—analysis of its role in *Drosophila* tracheal morphogenesis. *Dev Biol*. 2005; 288:179–193. [PubMed: 16277981]
11. Luschign S, Batz T, Armbruster K, Krasnow MA. serpentine and vermiform encode matrix proteins with chitin binding and deacetylation domains that limit tracheal tube length in *Drosophila*. *Curr Biol*. 2006; 16:186–194. [PubMed: 16431371]
12. Wang S, et al. Septate-junction-dependent luminal deposition of chitin deacetylases restricts tube elongation in the *Drosophila* trachea. *Curr Biol*. 2006; 16:180–185. [PubMed: 16431370]
13. Paul SM, Ternet M, Salvaterra PM, Beitel GJ. The Na<sup>+</sup>/K<sup>+</sup> ATPase is required for septate junction function and epithelial tube-size control in the *Drosophila* tracheal system. *Development*. 2003; 130:4963–4974. [PubMed: 12930776]
14. Behr M, Riedel D, Schuh R. The claudin-like megatrachea is essential in septate junctions for the epithelial barrier function in *Drosophila*. *Dev Cell*. 2003; 5:611–620. [PubMed: 14536062]
15. Nelson KS, Furuse M, Beitel GJ. The *Drosophila* Claudin Kune-kune is required for septate junction organization and tracheal tube size control. *Genetics*. 2010; 185:831–839. [PubMed: 20407131]
16. Paul SM, Palladino MJ, Beitel GJ. A pump-independent function of the Na,K-ATPase is required for epithelial junction function and tracheal tube-size control. *Development*. 2007; 134:147–155. [PubMed: 17164420]
17. Thomas SM, Brugge JS. Cellular functions regulated by Src family kinases. *Annu Rev Cell Dev Biol*. 1997; 13:513–609. [PubMed: 9442882]
18. Marx M, Warren SL, Madri JA. pp60(c-src) modulates microvascular endothelial phenotype and in vitro angiogenesis. *Exp Mol Pathol*. 2001; 70:201–213. [PubMed: 11417999]
19. Sweeney WE Jr, von Vigier RO, Frost P, Avner ED. Src inhibition ameliorates polycystic kidney disease. *J Am Soc Nephrol*. 2008; 19:1331–1341. [PubMed: 18385429]
20. Schwartzberg PL, et al. Rescue of osteoclast function by transgenic expression of kinase-deficient Src in src<sup>-/-</sup> mutant mice. *Genes Dev*. 1997; 11:2835–2844. [PubMed: 9353253]
21. Kaplan KB, Swedlow JR, Morgan DO, Varmus HE. c-Src enhances the spreading of src<sup>-/-</sup> fibroblasts on fibronectin by a kinase-independent mechanism. *Genes Dev*. 1995; 9:1505–1517. [PubMed: 7541382]
22. Pedraza LG, Stewart RA, Li DM, Xu T. *Drosophila* Src-family kinases function with Csk to regulate cell proliferation and apoptosis. *Oncogene*. 2004; 23:4754–4762. [PubMed: 15107833]
23. Shindo M, et al. Dual function of Src in the maintenance of adherens junctions during tracheal epithelial morphogenesis. *Development*. 2008; 135:1355–1364. [PubMed: 18305002]

24. Shiga Y, Tanaka-Matakatsu M, Hayashi S. A nuclear GFP/ $\beta$ -galactosidase fusion protein as a marker for morphogenesis in living *Drosophila*. *Development, Growth & Differentiation*. 1996; 38:99–106.
25. Takahashi M, Takahashi F, Ui-Tei K, Kojima T, Saigo K. Requirements of genetic interactions between Src42A, armadillo and shotgun, a gene encoding E-cadherin, for normal development in *Drosophila*. *Development*. 2005; 132:2547–2559. [PubMed: 15857910]
26. Padash-Barmchi M, Browne K, Sturgeon K, Jusiak B, Auld VJ. Control of Gliotactin localization and levels by tyrosine phosphorylation and endocytosis is necessary for survival of polarized epithelia. *J Cell Sci*. 2010; 123:4052–4062. [PubMed: 21045109]
27. LeClaire LL 3rd, Baumgartner M, Iwasa JH, Mullins RD, Barber DL. Phosphorylation of the Arp2/3 complex is necessary to nucleate actin filaments. *J Cell Biol*. 2008; 182:647–654. [PubMed: 18725535]
28. Aspenstrom P, Richnau N, Johansson AS. The diaphanous-related formin DAAM1 collaborates with the Rho GTPases RhoA and Cdc42, CIP4 and Src in regulating cell morphogenesis and actin dynamics. *Exp Cell Res*. 2006; 312:2180–2194. [PubMed: 16630611]
29. Matussek T, et al. The *Drosophila* formin DAAM regulates the tracheal cuticle pattern through organizing the actin cytoskeleton. *Development*. 2006; 133:957–966. [PubMed: 16469972]
30. Matussek T, et al. Formin proteins of the DAAM subfamily play a role during axon growth. *J Neurosci*. 2008; 28:13310–13319. [PubMed: 19052223]
31. Tominaga T, et al. Diaphanous-related formins bridge Rho GTPase and Src tyrosine kinase signaling. *Mol Cell*. 2000; 5:13–25. [PubMed: 10678165]
32. Young KG, Copeland JW. Formins in cell signaling. *Biochim Biophys Acta*. 2010; 1803:183–190. [PubMed: 18977250]
33. Segalen M, Bellaiche Y. Cell division orientation and planar cell polarity pathways. *Semin Cell Dev Biol*. 2009; 20:972–977. [PubMed: 19447051]
34. Ang SF, Zhao ZS, Lim L, Manser E. DAAM1 is a formin required for centrosome re-orientation during cell migration. *PLoS One*. 2010; 5

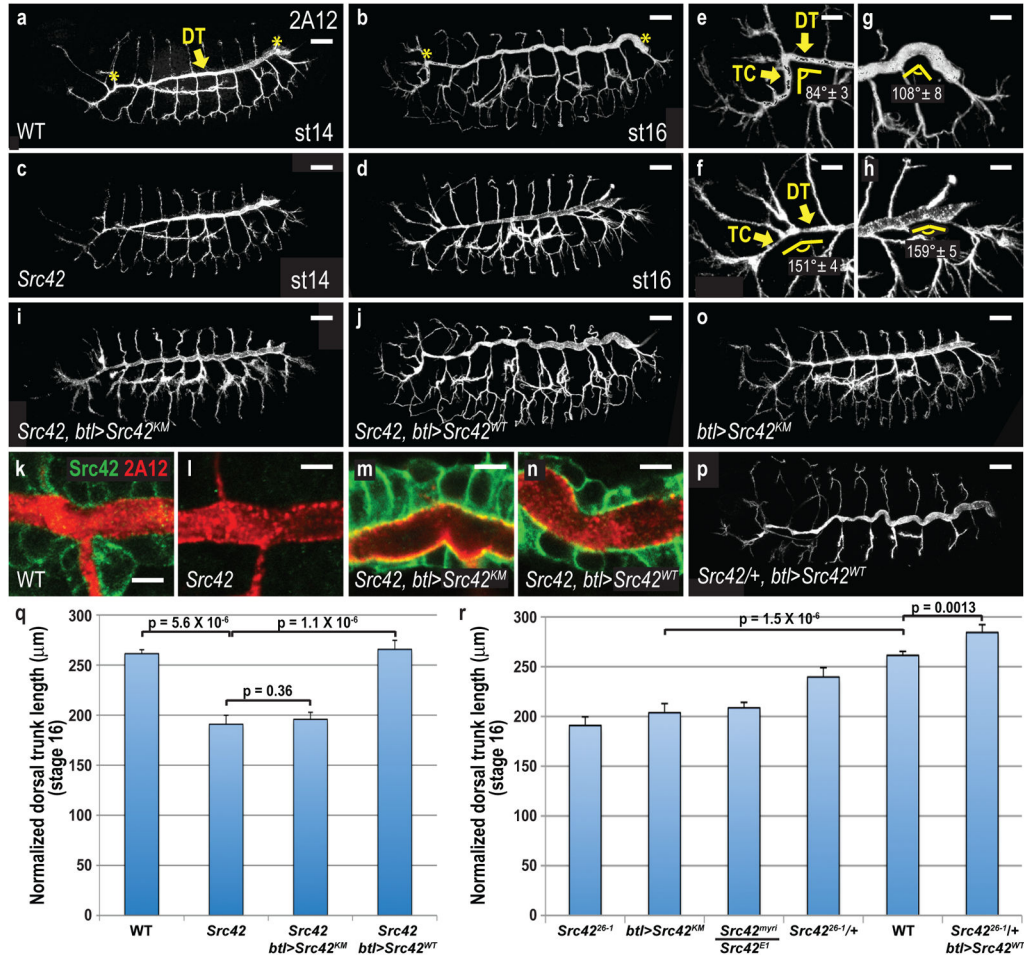


**Figure 1. *Src42* acts autonomously to control tracheal tube length**

(a–d) The dorsal trunk (DT, arrow) of *Src42* null mutant embryos appears normal at early embryonic stage 14 (a, c), but is dramatically shorter than WT by stage 16 (b, d). Asterisks indicate endpoints for DT measurements. Lumens in a–o and p visualized by staining for 2A12 antigen. (e, f) DT shortening increases the angle between the anterior transverse connective (TC) and the DT in *Src42* mutants (e, f) ( $n = 5$ ,  $p = 6 \times 10^{-9}$ ). (g, h) The angle of the posterior ventral curve is also increased in *Src42* mutants (g, h) ( $n = 5$ ,  $p = 1 \times 10^{-5}$ ). (i, j) *Src42* kinase activity is required for DT elongation, since tracheal-specific expression (*btl-Gal4<sup>24</sup>*) of a WT *Src42* transgene (*Src42<sup>WT</sup>*) (i) but not a kinase-dead form of *Src42* (*Src42<sup>KM</sup>*) fully rescues *Src42* DT elongation (j). (k–n) In WT embryos, *Src42* is found throughout the cell periphery of tracheal cells (k). *Src42* mutants completely lack *Src42* labeling. (l). The *Src42<sup>KM</sup>* and *Src42<sup>WT</sup>* transgenes are expressed at similar levels in the trachea of *Src42* mutants (m, n). (o) *Src42<sup>KM</sup>* acts as a dominant negative in the tracheal system, as its over-expression inhibits DT elongation. (p) Conversely, over-expression of *Src42<sup>WT</sup>* in the tracheal system of *Src42* heterozygotes over elongates tracheal tubes. (q) Quantification of DT length in *Src42* rescue experiments reveals statistically significant differences between *Src42<sup>KM</sup>* and *Src42<sup>WT</sup>*. (r) Allelic series using loss- and gain-of-function alleles and transgenes reveals that tracheal length correlates with *Src42* levels. Note

that over-expression of Src42<sup>KM</sup> results in tracheal tubes that are comparable in length to null alleles. For q and r, error bars represent standard deviation, all p values are determined using Student's t-tests, and n = 5 for all samples. Scale bars: 20  $\mu\text{m}$  for a–d, i, j, o, p; 10  $\mu\text{m}$  for e–h; 5  $\mu\text{m}$  for k–n.

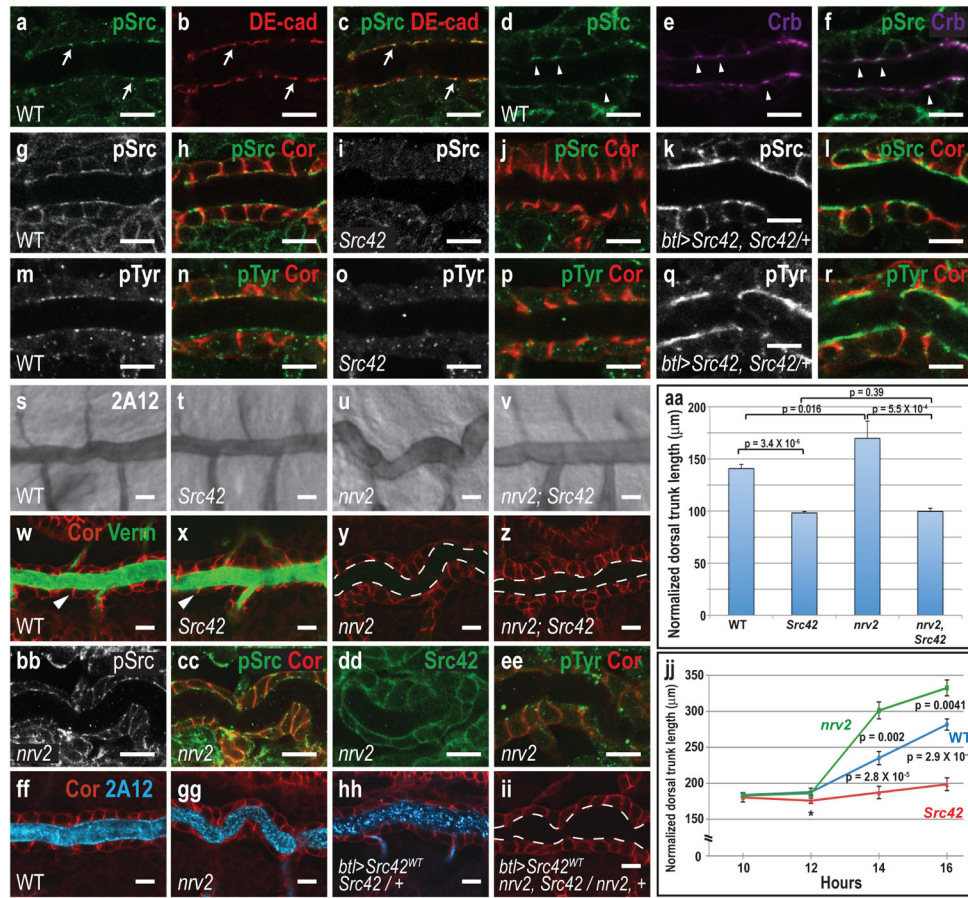


**Figure 2. *Src42* acts independently of the aECM-based tube size control pathway**  
**(a–c)** Activated Src42 (pSrc) colocalizes with DE-cadherin (DE-cad) at the adherens junction (AJ). **(d–f)** pSrc shows some partial overlap with Crb at the subapical membrane. **(g, h)** Activated Src localizes apical to the septate junction (SJ), which is labeled with Coracle (Cor), a canonical SJ marker. **(i, j)** *Src42* mutants show essentially no pSrc labeling, indicating that the pSrc antibody is specific for activated Src42. **(k, l)** Over-expression of Src42 results in a dramatic increase in pSrc. **(m–r)** Labeling for phosphotyrosine (pTyr) shows that most tyrosine-phosphorylated proteins also localize apical to SJs (m, n). Src42 is required for much of the tyrosine phosphorylation at the apical membrane (m–p) and Src42 over-expression increases apical pTyr (q, r). **(s–v)** *Src42* is epistatic to the aECM/SJ pathway, since *Src42* mutants fully suppress tracheal over-elongation in aECM/SJ mutants, such as *nrv2*. **(w–z)** *Src42* mutations do not disrupt SJ organization (note localized red Cor staining at the apical region of the lateral membranes, arrowheads in w and x) or Verm secretion (green luminal staining) and suppress *nrv2* tube elongation without restoring SJ organization (note diffuse Cor staining) or Verm secretion (note the lack of Verm staining) (y, z). Dashed lines mark the apical surface. **(aa)** The DT of *Src42*, *nrv2* double mutants are the same length as *Src42* single mutants. The length of the DT between TC5 and TC10 was measured because the over-elongation of aECM/SJ mutants is most apparent in the posterior DT. Error bars represent standard deviation. p values are from Student's t-tests. For all samples, n = 5. **(bb–ee)** *nrv2* null mutants do not show obvious changes in the levels

or localization of pSrc (bb, cc) Src42 (dd), or pTyr (ee), indicating that the aECM does not directly regulate Src42. See Figure 2 for WT comparisons. **(ff–ii)** Over-expression of Src42 in a *nrv2* background results in a loss of luminal 2A12 and tracheal tubes that are cystic (ii). The enhanced phenotype indicates that *Src42* and *nrv2* are unlikely to function in the same genetic pathway. Dashed lines mark the apical cell surface. **(jj)** Measurement of DT length in WT, *Src42*, and *nrv2* animals at two hour intervals shows that the DT of WT, *nrv2*, and *Src42* are the same length at 10 h, just after tracheal metameres fuse ( $p = 0.46$  for WT and *Src42*,  $p = 0.78$  for WT and *nrv2*). However, by 12 h, *Src42* DTs are shorter than WT (\*,  $p = 0.044$ ), while *nrv2* mutants are not different from WT ( $p = 0.69$ ). *nrv2* mutants do not show significantly increased tube length compared to WT embryos until 12 h. Error bars represent standard deviation. p values are from Student's t-tests. For hour 14 (stage 16),  $n = 5$  for each genotype. For all other time points,  $n = 3$  for each genotype. Scale bars: 10 $\mu$ m for a–z, bb–ii.

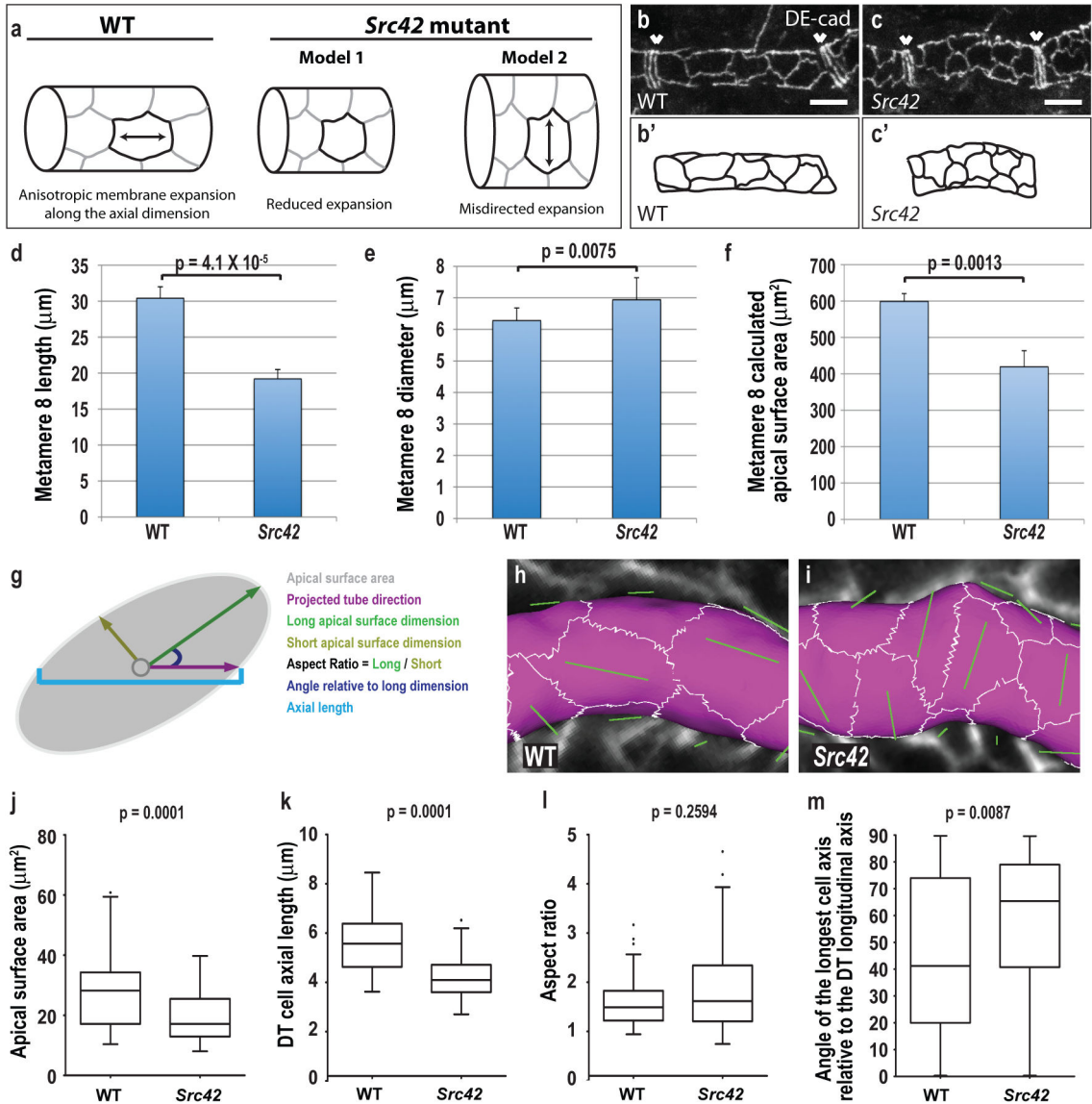


**Figure 3. *Src42* is required for orienting anisotropic apical surface expansion along the longitudinal axis of tracheal tubes**

(a) Two models that could account for shortened DTs in *Src42* mutants. Model 1, apical surface expansion is reduced, preventing anisotropic growth along the axial dimension. Model 2, apical surface expansion is misdirected along the circumferential dimension, producing shorter but fatter tubes. (b, c) Confocal projections of metamere 8 in WT (b) and *Src42* (c) embryos labeled for DE-cadherin (DEcad) show that *Src42* cells appears “shorter” than WT along the longitudinal axis of the tube. Arrowheads mark metamere ends. Scale bar: 5µm for b, c. (b',c') Cell tracings of b, c. (d,e) The length of metamere 8 (fusion cell to fusion cell) is shorter in *Src42* mutants than in WT, but diameter is increased. (f) The calculated apical surface area of *Src42* metamere 8 is smaller than WT. For d–f, error bars represent standard deviation. p values are from Student’s t-test. For all samples, n = 5. (g) Schematic showing the parameters measured for reconstructed cells. For details, see

Materials and Methods. **(h, i)** A representative reconstruction of the apical surface of WT **(h)** and *Src42* **(i)** metamere 8 cells showing the long axis of each cell (green line). The long axes of *Src42* cells are misoriented towards the circumferential direction. **(j)** The median apical surface area of individual *Src42* cells is smaller than WT. **(k)** The median length of cells along the longitudinal axis of the DT is shorter in *Src42* than WT. **(l)** The median aspect ratio of WT and *Src42* cells is not statistically different. **(m)**. The median angle of the longest cell axis relative to the DT longitudinal axis is increased in *Src42* mutants. For j–m, black bars represent the median, boxes delineate the upper and lower quartiles, whiskers indicate the highest and lowest values within 1.5 times the interquartile range, and dots represent outliers. p values are from Mann-Whitney *U* tests. For all box plots, cells were pooled from 4 embryos for n values of 57 cells (WT) and 67 cells (*Src42*).

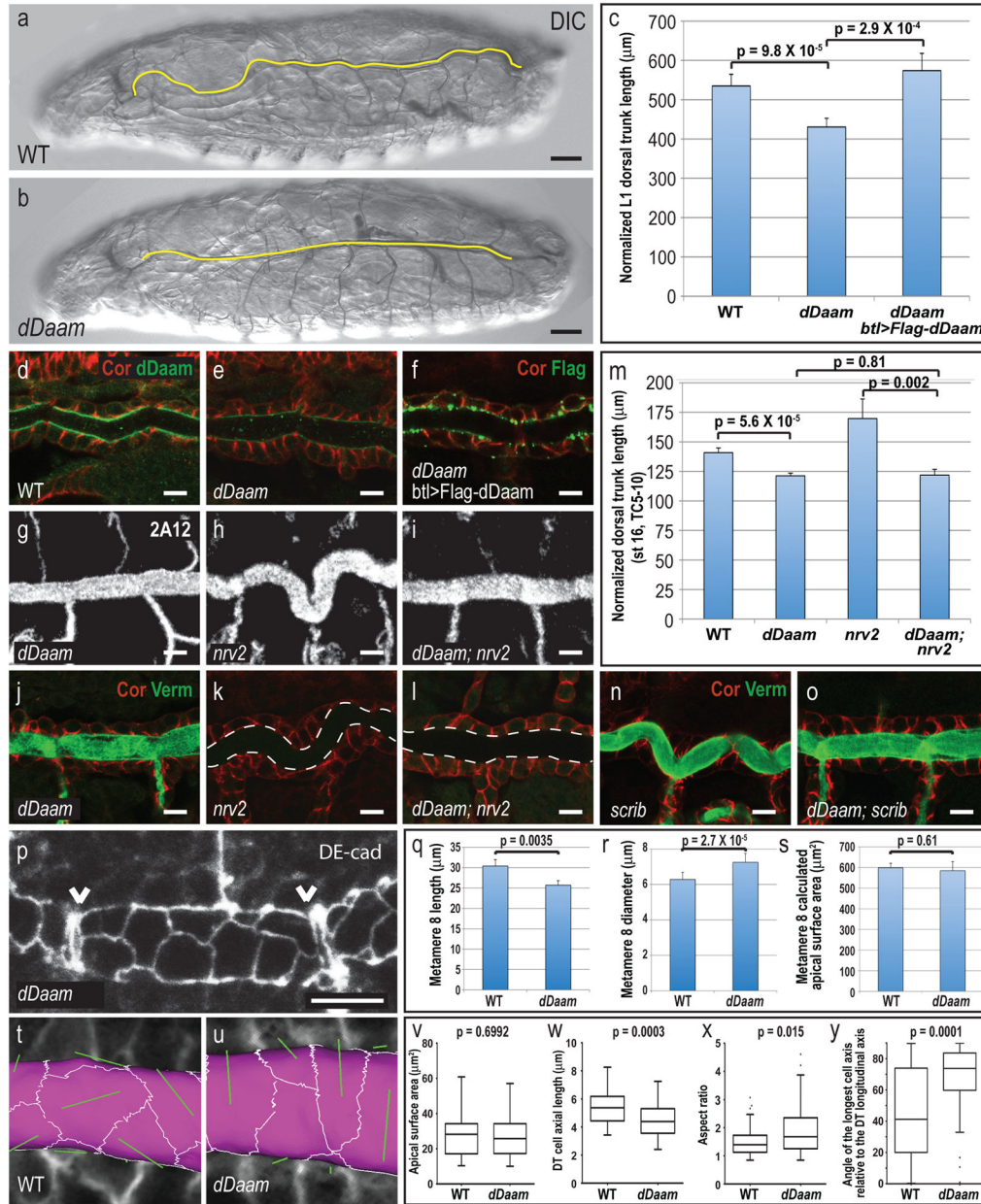


**Figure 4. *dDaam* is required for tracheal tube elongation**  
 (a, b, c) The DT (yellow line) of *dDaam* first instar larvae is shorter than WT. (c) Tracheal specific expression of a Flag-tagged *dDaam* construct (Flag-*dDaam*) can fully rescue the *dDaam* elongation defect. Error bars represent standard deviation. p values are from Student's t-tests. For WT, n = 6, for *dDaam*, n = 8, and for Flag-*dDaam* rescue, n = 7. (d) *dDaam* is localized at the apical surface of WT tracheal cells. (e) *dDaam* labeling is greatly reduced in *dDaam* mutants. (f) The Flag-*dDaam* rescue construct localizes correctly to the apical surface. (g–l) *dDaam* can suppress the DT over-elongation of *nrv2* (m) The DT of *dDaam; nrv2* double mutants is the same length as *dDaam* single mutants. Error bars represent standard deviation, n = 5 for all samples. (n, o) *dDaam* can suppress the over-elongation of *scrib* mutants. (p) Confocal projections of metamer 8 in *dDaam* embryos

labeled for DE-cad. **(q, r)** Metamere 8 of *dDaam* mutants is shorter in length (q) but larger in diameter (r) than WT. **(s)** Unlike *Src42* mutants, the calculated apical surface area of *dDaam* metamere 8 is not different from WT. For m, q–s error bars represent standard deviation, p values are from Student's t-test, n = 5. **(t, u)** Representative reconstruction of the apical surface of WT (t) and *dDaam* (u) metamere 8 cells shows that the long axis (green line) of *dDaam* cells is oriented circumferentially. **(v)** The median apical surface area of individual *dDaam* tracheal cells is not significantly different from WT. **(w)** The median length of cells along the longitudinal axis of the DT is shorter in *dDaam* cells than WT. **(x)** The median aspect ratio of *dDaam* cells is slightly larger than WT. **(y)** However, *dDaam* cells are misoriented along the circumferential direction. For v–x, black bars represent the median, boxes delineate the upper and lower quartiles, whiskers indicate the highest and lowest values within 1.5 times the interquartile range, and dots represent outliers. p values are from Mann-Whitney *U* tests. For all box plots, cells were pooled from 4 embryos for n values of 57 cells (WT) and 59 cells (*dDaam*). Scale bars: 40 $\mu$ m for a, b; 10 $\mu$ m for d–l, n–p.

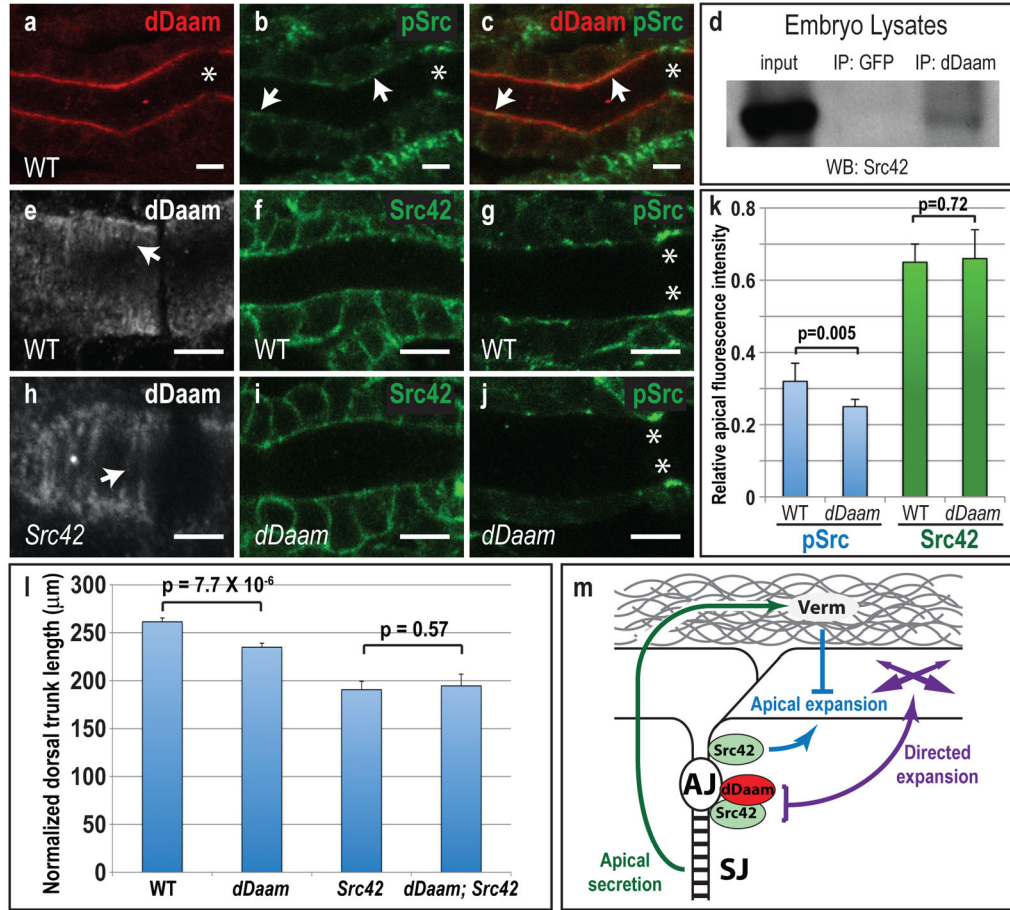


**Figure 5. dDaam functions with Src42 to control tube size**

(a–c) dDaam colocalizes with pSrc at the subapical membrane of DT cells (arrows, b, c). However, dDaam is not expressed in fusion cells (asterisks). (d) Src42 co-immunoprecipitates with dDaam from embryo lysates. The blot is representative of three independent experiments (entire blot is shown in Fig. S5g). Anti-GFP antibody was used as a negative control. (e–j) dDaam is enriched in apical circumferential rings (arrows in e and h) that run orthogonally to the length of the tube (e). In *Src42* mutants, dDaam still localizes to circumferential rings, but the rings are coarser and more broadly spaced (h). Images in e and h are superficial sections of the DT. Localization of Src42 is not affected in early stage 17 *dDaam* mutants (f, i). Nonetheless, early stage 17 *dDaam* mutants show a reduction in the levels of pSrc (g, j). Note that pSrc is not affected in fusion cells, where dDaam is not expressed (asterisks, j). Stage 17 *dDaam* embryos were imaged to account for maternal *dDaam*. (k) Quantification of apical pSrc (blue) and Src42 (green) levels in WT and *dDaam* early stage 17 DT cells shows that the levels of activated Src42 are reduced in *dDaam* mutants. (l) Measurement of *dDaam* and *Src42* mutant DTs show that both are shorter than WT. *dDaam; Src42* double mutants do not display a more severe elongation defect than *Src42* single mutants. For k and l, error bars represent standard deviation, p values are from Student’s t-test, and n = 5 for all samples (m) A model for the interactions of aECM and the Src42/dDaam in controlling lumen size. Src42 is required for apical surface growth and both

Src42 and dDaam direct growth along the longitudinal axis. aECM restricts tube length. Note that Src and dDaam are shown at the AJ, but the location of the pools of Src and dDaam that control the amount and direction of growth are not known. Scale bars: 10 $\mu$ m for a–c, f, g, i, j; 5 $\mu$ m for e, h.

Author Manuscript

Author Manuscript

Author Manuscript

Author Manuscript